Numerical Study on Propeller Slipstream Effects on Objects at Low Reynolds Number

Report Number: R22EACA43
Subject Category: JSS Inter-University Research
URL: https://www.jss.jaxa.jp/en/ar/e2022/20755/

Responsible Representative

Keiichi Kitamura, Associate professor, Yokohama National University

Contact Information

Yoshikatsu Furusawa(furusawa-yoshikatsu-vz@ynu.jp)

Members

Yoshikatsu Furusawa, Keiichi Kitamura, Keita Suzuki, Shunya Sakatsume

Abstract

As a new form of a Mars exploration vehicle, research and development of a propeller-driven Mars airplane are progressing. Because the low atmospheric density on Mars causes the flow around the Mars airplane at low Reynolds numbers, the flow field around the Mars airplane differs from airplanes flying in the Earth's atmosphere. Besides, it is known that the propeller slipstream interacts with the fixed-wing and the fuselage and affects their aerodynamic characteristics. These interactions are important aerodynamic phenomena on the Earth airplane like eVTOL, because they arise at high Reynolds number. In the present study, we conduct numerical simulations and intend to clarify the unsteady effects of propeller slipstream on the fixed-wing and the fuselage at a wide range from low Reynolds number to high Reynolds number regions.

Reasons and benefits of using JAXA Supercomputer System

We used JSS3 to perform large-scale three-dimensional numerical simulations using the flow analysis solver "rFlow3D" , "FaSTAR" and "FaSTAR-Move" developed by JAXA. JSS3 can perform fast and multiple calculations.

Achievements of the Year

In this work, unsteady numerical calculations simulating the wind tunnel experiments conducted at Tohoku University were carried out. Comparing flow around the wind-tunnel scale model (incompressible flow) and the actual scale model (compressible flow around the propeller), we investigated compressible effects around the propeller on the aerodynamics characteristics of the fixed wing within the propeller slipstream during the actual flight on Mars. The Propeller advance ratio and the Reynolds number on both scales are the same value; J = 0.8 and Re = 30,000. The propeller rotation speed is n = 4,500, and the angle of attack was set to 4 deg. In this case, the blade tip Mach numbers are M_{tip} = 0.10 for the wind-tunnel scale model and M_{tip} = 0.52 for the actual scale model.

Figure 1 shows the instantaneous Q-criterion fields (when the propeller is vertically upward) at the 63% position of the propeller span. Several vortices are shed from the separated shear layer over the blade in the wind tunnel scale model, while vortices are not formed in the actual scale model, suggesting compressibility stabilized the separated shear layer. Figure 2 shows the azimuthal normal force coefficient distributions acting on the blade within one propeller rotation. The azimuthal distribution of the actual scale exhibits weaker variation than that of the wind tunnel scale model. Hence, it was revealed that the compressibility stabilized the separated shear layer over the blade, leading to insignificant propeller vibration. Investigations of their effects on the fixed-wing, which is within the propeller slipstream, are ongoing.

In this work, unsteady calculations simulating level flight of the eVTOL at the high Reynolds number region were also carried out. Solving for the flow field between the propellers and fuselage, we investigated the aerodynamic interactions arising between them. The uniform flow velocity is M = 0.1 and the Reynolds number is Re = 3,700,000. The propeller rotation speed is n = 1800 rpm and the blade setting angle is 11 deg.

Figure 3 shows the instantaneous Q-criterion isosurface and surface pressure coefficient. The surface pressure is low along the wingtip vortexes generated by the propellers. Hense, it was revealed that the effect of the wingtip vortex on aerodynamic interactions. Investigations of the three-way aerodynamic interavtion, including not only the fuselage and propellers but also the fixed wing, are ongoing.

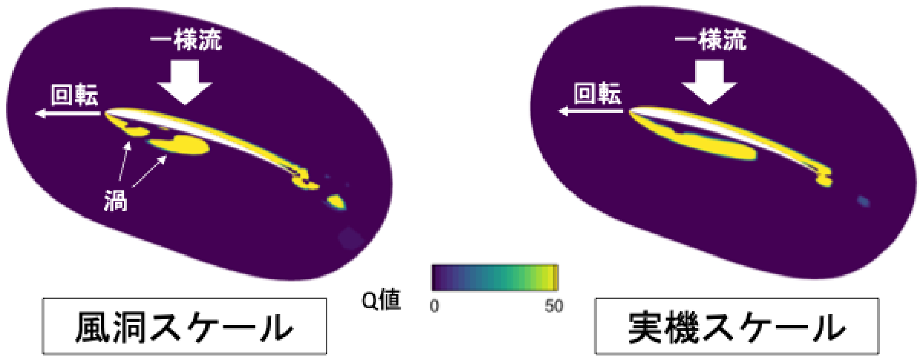

Fig. 1: Instantaneous Q-criterion fields (when propeller is vertically upward) at 63% position of propeller span.

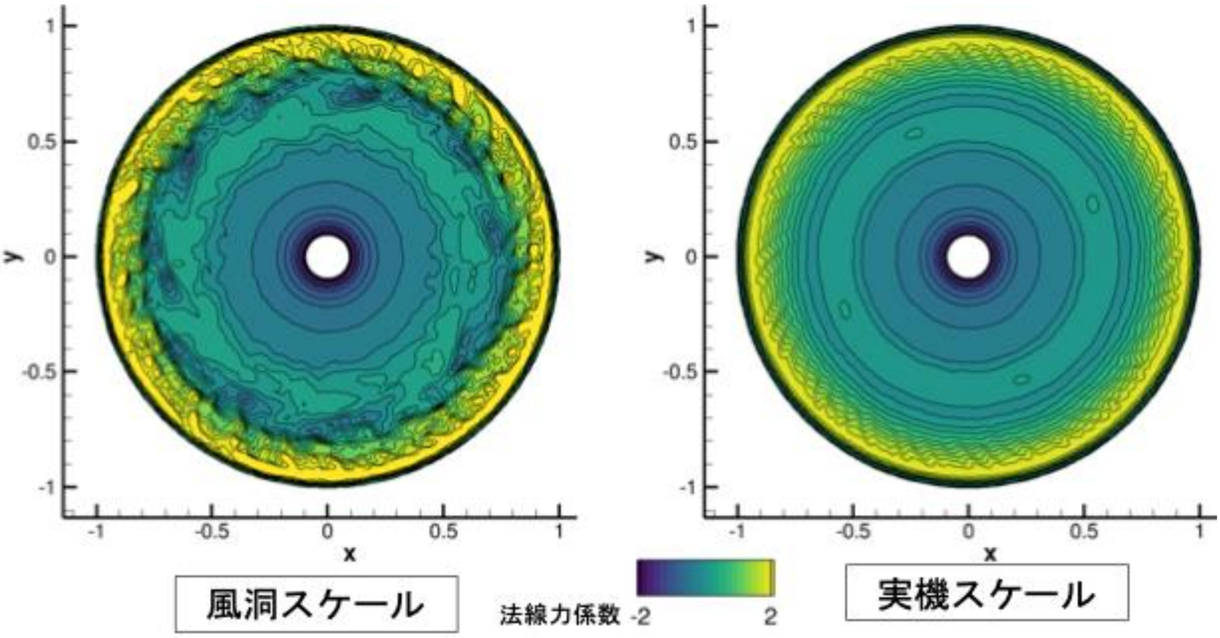

Fig. 2: Azimuthal normal force coefficient distributions acting on blade within one propeller rotation.

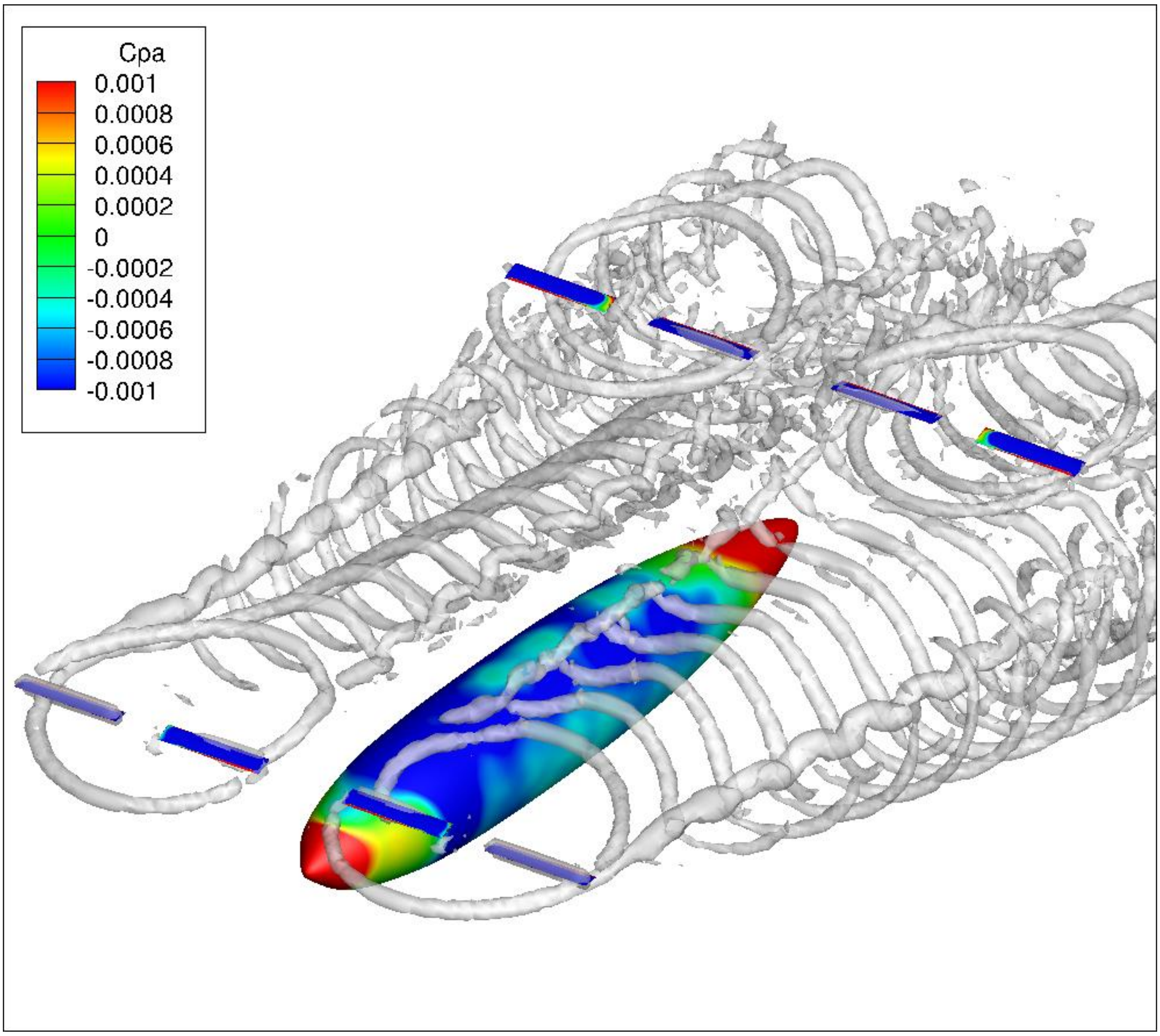

Fig. 3: Instantaneous Q-criterion isosurface and surface pressure coefficient on the fuselage

Publications

- Peer-reviewed papers

Furusawa, Y., Kitamura, K., "Stability effect of multidimensional velocity components in numerical flux SLAU," International Journal for Numerical Methods in Fluids, 2023 (Accepted).

- Oral Presentations

Furusawa, Y. and Kitamura, K., "Roles of Multi-Dimensional Velocity Components in All-Speed Numerical Flux SLAU," AIAA Paper 2022-4033, 2022.

Furusawa, Y. and Kitamura, K., "Stability Effect of Multi-dimensional Velocity Component on Compressible All-speed Scheme, Part II: Investigation on More Extensive Mach Numbers," 36th Computational Fluid Dynamics Symposium, 2022.

Keita, S., "Numerical analysis of the effect of rotor position on eVTOL aircraft aerodynamics," 60th aircraft symposium, 2022.

- Poster Presentations

Furusawa, Y., Kitamura, K., Ikami, T., Okawa, M., and Nagai, H., "Numerical Study on Propeller Scale Effect on Flow Field around Blade," 19th International Conference on Flow Dynamics, 2022.

Keita, S., "Numerical analysis of the effect of rotor position on eVTOL aircraft aerodynamics," 2022 JSAE Annual Congress (Spring), 2022.

Usage of JSS

- **Computational Information**

Process Parallelization Methods	MPI
Thread Parallelization Methods	OpenMP
Number of Processes	36 - 1440
Elapsed Time per Case	720 Hour(s)

- **JSS3 Resources Used**

Fraction of Usage in Total Resources[*1](%): 0.25

Details

Computational Resources		
System Name	CPU Resources Used (core x hours)	Fraction of Usage[*2](%)
TOKI-SORA	2,086,241.03	0.09
TOKI-ST	1,193,760.00	1.19
TOKI-GP	0.00	0.00
TOKI-XM	0.00	0.00
TOKI-LM	16,157.76	1.08
TOKI-TST	0.33	0.00
TOKI-TGP	0.00	0.00
TOKI-TLM	0.00	0.00

File System Resources		
File System Name	Storage Assigned (GiB)	Fraction of Usage[*2] (%)
/home	20.33	0.02
/data and /data2	25,720.00	0.20
/ssd	1,876.67	0.26

Archiver Resources		
Archiver Name	Storage Used (TiB)	Fraction of Usage[*2] (%)
J-SPACE	6.07	0.03

[*1]: Fraction of Usage in Total Resources: Weighted average of three resource types (Computing, File System, and Archiver).

[*2]: Fraction of Usage：Percentage of usage relative to each resource used in one year.

- **ISV Software Licenses Used**

ISV Software Licenses Resources		
	ISV Software Licenses Used (Hours)	Fraction of Usage[*2] (%)
ISV Software Licenses (Total)	5,237.39	3.64

[*2]: Fraction of Usage：Percentage of usage relative to each resource used in one year.